

# The Centaurus Group and the Outer Halo of NGC 5128: Are they Dynamically Connected?

Kristin A. Woodley

*Department of Physics & Astronomy, McMaster University, Hamilton ON L8S 4M1*

woodleka@physics.mcmaster.ca

## ABSTRACT

NGC 5128, a giant elliptical galaxy only  $\sim 4$  Mpc away, is the dominant member of a galaxy group of over 80 probable members. The Centaurus group provides an excellent sample for a kinematic comparison between the halo of NGC 5128 and its surrounding satellite galaxies. A new study, presented here, shows no kinematic difference in rotation amplitude, rotation axis, and velocity dispersion between the halo of NGC 5128, determined from over  $\sim 340$  of its globular clusters, and those of the Centaurus group as a whole. These results suggest NGC 5128 could be behaving in part as the inner component to the galaxy group, and could have begun as a large initial seed galaxy, gradually built up by minor mergers and satellite accretions, consistent with simple cold dark matter models. The mass and mass-to-light ratios in the B-band, corrected for projection effects, are determined to be  $(1.3 \pm 0.5) \times 10^{12} M_{\odot}$  and  $52 \pm 22 M_{\odot}/L_{\odot}$  for NGC 5128 out to a galactocentric radius of 45 kpc, and  $(9.2 \pm 3.0) \times 10^{12} M_{\odot}$  and  $153 \pm 50 M_{\odot}/L_{\odot}$  for the Centaurus group, consistent with previous studies.

*Subject headings:* galaxies: elliptical and lenticular, cD — galaxies: individual (NGC 5128) — galaxies: kinematics and dynamics — globular clusters: general

## 1. Introduction

The study of galaxy groups can provide essential insight into galaxy formation, particularly because many groups are much less dynamically evolved than rich clusters and thus are closer to their earliest conditions. The density of formation environment affects the dynamical evolution of galaxies; for example, the luminosity and color distributions of galaxies differ in field versus group environments (Girardi et al. 2003). Furthermore, for groups with large central members, the properties of the central galaxy correlate with properties of their

satellite galaxies, such as the satellite-type fraction found in the group (Weinmann et al. 2006), the alignment of satellite galaxies preferentially along the dominant galaxy’s major axis (Yang et al. 2006; Brainerd 2005; Zentner et al. 2005), and the rotation of satellite galaxies in the same direction as the host halo (Warnick & Knebe 2006).

The connections between the centrally dominant galaxy in a group environment and its surrounding satellite galaxies raise the question whether there might be a more direct kinematic connection between them as well. Kinematic similarities between the group and its brightest group member would be consistent with both cold dark matter models, suggesting the central giant and its satellite group are part of the same large-scale structure, and the hierarchical formation scenario, whereby the central giant would build up by accretion of satellites in the group.

NGC 5128 is an E/S0 giant galaxy in the positional and dynamical center of the Centaurus group of galaxies. Its remarkably close proximity (just 4 Mpc distant) also provides a genuinely rare opportunity to study and compare the dynamics of the halo of NGC 5128 with the dynamics of the surrounding group at a level of detail that is difficult elsewhere.

The Centaurus group consists of 25 confirmed galaxy members (Karachentsev et al. 2006), 13 of which have radial velocity measurements used in this kinematic study; see Figure 1. Within a projected distance of  $\sim 1$  Mpc from NGC 5128 lies NGC 5236 (M83). NGC 5236 is a dominant spiral galaxy surrounded by 9 other confirmed members within the M83 group. Surrounding these two systems are 53 smaller galaxies that do not have confirmed membership in either the Centaurus group or the M83 group. Therefore the bounds separating these two groups are still quite uncertain, and it has been suggested that these two systems create a dumbbell system, similar to our own Milky Way and M31 (Karachentsev et al. 2006).

Only one other kinematic comparison between the halo of a dominant galaxy and its surrounding satellite galaxies (M87 in the Virgo cluster) has been presented in the literature (Côté et al. 2001). Virgo is a much more dynamically evolved environment than the Centaurus group. The Centaurus group, therefore, provides the chance to carry the comparison a step further than just alignments of satellites and simple number statistics by looking at an environment closer to its initial structure.

## 2. Kinematics

NGC 5128 has many hundreds of globular clusters (GCs) that can be used to define its halo kinematics and dynamics. The most recent studies (M. Beasley et al. 2006, in

preparation; Woodley, Harris, & Harris 2005; Peng, Ford, & Freeman 2004) now raise the confirmed globular cluster (GC) membership to  $\sim 340$  members with known radial velocities, which make up the sample used in this paper (this list includes  $\sim 100$  new clusters to be published in M. Beasley et al. (2006, in preparation), written in tandem to this study). A full catalogue of all GCs in NGC 5128, along with radial velocities and photometry will be published in K. Woodley (2006, in preparation). The Centaurus group and neighbouring M83 group, have many smaller galaxies with radial velocity measurements. This combined material enables a kinematic and dynamic comparison between the brightest group member and its satellite group.

The kinematics of both the globular cluster system (GCS) of NGC 5128 and the Centaurus group of galaxies are defined using the normal condition

$$v_r(\Theta) = v_{sys} + \Omega R \sin(\Theta - \Theta_o) \quad (1)$$

(e.g. Richtler et al. 2004; Côté et al. 2001) where  $v_r$  is the observed radial velocity of the object in the system,  $v_{sys}$  is the systemic velocity,  $R$  is the projected radial distance of each object from the center of the system, and  $\Theta$  is the projected azimuthal angle of the object measured in degrees East of North. The quantities obtained by applying this equation to the system, with the known  $v_{sys} = 541 \text{ km s}^{-1}$  for NGC 5128 (Hui et al. 1995) held constant, are  $\Theta_o$ , the rotation axis of the system measured, and the product  $\Omega R$ , the rotation amplitude of the objects in the system.

The projected velocity dispersion is calculated using the maximum likelihood dispersion estimator described by Pryor & Meylan (1993),

$$\sum_{i=1}^N \frac{(v_i - v_{sys})^2}{(\sigma_v^2 + \sigma_{v_{r_i}}^2)} = \sum_{i=1}^N \frac{1}{(\sigma_v^2 + \sigma_{v_{r_i}}^2)} \quad (2)$$

where  $N$  is the number of clusters in the sample,  $v_i$  is the cluster's radial velocity *after subtraction of the rotational component*, and  $\sigma_{v_{r_i}}$  is the uncertainty in the velocity measurement.  $\sigma_v$  is the projected velocity dispersion determined by iterating through values of  $\sigma_v$  to find the equality of Equation 2. The systemic velocity is again held constant at  $541 \text{ km s}^{-1}$ . The uncertainties were calculated from the variance of the dispersion using Equations 6, 8, 9, & 10 from Pryor & Meylan (1993).

## 2.1. The Globular Cluster System of NGC 5128

The kinematic condition of Equation 1 was applied to the GCS of NGC 5128. A total of 343 GCs with radial velocity membership in NGC 5128 have been used in the kinematic

determination. The radial velocities used are the weighted averages from all previous measurements studies of NGC 5128 and are described completely in K. Woodley et al. (2006, in preparation). The GCs were assigned weights in the kinematic fitting by considering two components to their associated uncertainties: the individual observational uncertainty in  $v_r$ , and the random velocity component of the GCS evident by the large dispersion in the confirmed GC velocities. In almost all cases, this latter term dominates, leaving the clusters with very similar weights.

The fitted values of  $\Omega R$  and  $\Theta_o$  were determined for projected galactocentric radial bins with inner and outer radii listed in column 1 of Table 1. Successive columns give the mean radius and the outer radius in kpc assuming a distance of 3.9 Mpc, the number of GCs, the rotation amplitude in  $\text{km s}^{-1}$ , the rotation axis of the GCs in each circular radial bin in degrees East of North, the velocity dispersion in  $\text{km s}^{-1}$ , the projected mass correction factor, the pressure supported component of mass, the rotationally supported component of mass, and the total mass (see Section 3 for the mass discussion).

The radial bin 0-5 kpc has a different rotation solution from bins 5-10, 10-15, 15-25, 25-50, and 0-50 kpc. In bin 0-5 kpc, these GCs nominally rotate around a similar rotation axis as the remaining bins, but in an opposing direction. This result may be real for this innermost radial bin since it contains 55 clusters distributed evenly in angle over that portion of the sky (see Figure 2). However, the rotation amplitude is scarcely different from zero, and the system is clearly dominated by internal random motion there.

Fig. 2 displays the sine curve fits defined by Equation 1. Beyond a galactocentric distance of 15 kpc, the observational bias of the detections (most of the known outer clusters lie along the isophotal major axis of the galaxy, which is where previous searches have mainly concentrated) is evident by a clear lack of known GCs near the photometric minor axis of  $\Theta = 119$  and  $299 \pm 5^\circ$  (Dufour et al. 1979). This bias leads to higher uncertainties in the determined kinematic quantities in these outer regions. Nevertheless, it is notable that the kinematics of the metal-poor and metal-rich populations of GCs in NGC 5128 do not show any extreme differences in the outer-halo region and I treat them as a combined sample in the following discussion. Full details of the kinematic solutions of the metallicity sub-populations are discussed in K. Woodley et al. (2006, in preparation).

The velocity dispersion of the GCS ranges from 105 to 166  $\text{km s}^{-1}$ , and the entire system as a whole has a mean dispersion of  $123 \pm 6 \text{ km s}^{-1}$ . These results show striking resemblances to those of Peng, Ford, & Freeman (2004): from an earlier and smaller sample, they find the velocity dispersion of the GCs in NGC 5128 to range from 100 – 150  $\text{km s}^{-1}$  out to a projected radius of 50 kpc, with the largest dispersion at 20 kpc (see their Figure 20).

## 2.2. The Satellite Galaxies

The same kinematic analysis was applied to the Centaurus group of galaxies. NGC 5128, as the brightest member of the Centaurus group, was considered the center of mass of the system, and the surrounding small galaxies as its satellites.

The distances of the surrounding galaxies were taken from Table 2 of Karachentsev et al. (2006), while the distance to NGC 5128 itself, was assumed to be 3.9 Mpc from Rejkuba (2004). The positions and radial velocities of the galaxies were taken from Table 1 of Karachentsev et al. (2004). The rotation amplitude and rotation axis were determined for the confirmed galaxies with known radial velocities that are considered Centaurus group members; Karachentsev et al. (2006) have confirmed 13 members in the Centaurus group and 8 members in the M83 group with published radial velocities in Karachentsev et al. (2004).

Kinematic solutions were also determined for all satellite galaxies around NGC 5128, not just those with confirmed membership in Karachentsev et al. (2006), in two different ways. The first method has grouped the surrounding galaxies into two independent bins. Bin 1 contains the nearest 27 galaxies in projected radii to NGC 5128, excluding any confirmed members of the M83 group. Bin 2 contains the 28<sup>th</sup> to 53<sup>rd</sup> nearest galaxies to NGC 5128, again excluding any confirmed members of the M83 group. The results for the Centaurus group, M83 group, and the two independently binned samples are listed in Table 2. In all subsequent plots, the radial values plotted for the GCs, M83 group, Centaurus group, Bin 1, and Bin 2 are the mean positions of radii in the sample for the rotation amplitude, rotation axis, and velocity dispersion, while the data is plotted at the outermost radii in each bin for the mass plot.

The second method determines the same kinematics for the galaxies surrounding NGC 5128, beginning with the first 14 galaxies in projected radial distance. Successively adding one galaxy radially outward from NGC 5128 to the first 14 galaxies and recalculating the kinematic quantities was performed out to a maximum of 62 galaxies, *including M83 group members*, with results as shown in Table 3 (although only every third point is listed in Table 3, all points are plotted in subsequent figures)<sup>1</sup>. In all subsequent plots, the radial values plotted for the cumulative galaxy bins are the radial value of the last galaxy in the sample. Tables 2 & 3 list, in successive columns, the bin description in Table 2 or the number of galaxies included in the calculation in Table 3, the mean projected radius and

---

<sup>1</sup>The dwarf galaxy, Tucana was not included in the present analysis because of its large projected distance from NGC 5128.

outer projected radius in Table 2 and the outer projected radius in Table 3 of the sample in kpc, the rotation amplitude in  $\text{km s}^{-1}$ , the rotation axis in degrees East of North, the velocity dispersion in  $\text{km s}^{-1}$ , the volume density slope, the pressure supported mass, the rotationally supported mass, the total mass, the B-band luminosity in solar luminosity units, and mass-to-light ratio. There appears to be no significant kinematic difference within measurement uncertainty for all the subgroups of galaxies used in this study.

### 2.3. Kinematic Discussion

Figure 3 shows the rotation amplitude as a function of projected radius from the center of NGC 5128 for the GCs in NGC 5128, as well as the Centaurus group, Bin 1, Bin 2, and the cumulative galaxy bins including up to 62 galaxies surrounding NGC 5128. Figure 4 shows the rotation axis as a function of projected radius from NGC 5128.

The kinematic solution of the outer halo of NGC 5128, determined by its GC population, closely matches that of the satellite group. This suggests that the entire Centaurus group of galaxies could be thought of as an outward extension of its massive central galaxy; or conversely, that the halo of NGC 5128 behaves like an inward extension of the entire group. This result would be consistent with the idea that NGC 5128, starting from an initial (perhaps large) "seed" galaxy, could have built up from the accretions of many nearby small satellites that would have preferentially come in along the major axis of the group. Alternatively, if NGC 5128 formed from the merger of a *small* number of *large* galaxies (perhaps only 2 or 3 galaxies), it would not as easily explain the kinematic similarities since these few would be less likely to come together along this same axis.

Figure 5 shows the velocity dispersion as a function of projected radius from the center of NGC 5128, plotted for the same objects as Figs. 3 & 4. The cumulatively binned galaxies exhibit a similar range of velocity dispersion to the GCs in NGC 5128, from  $83 - 138 \text{ km s}^{-1}$ . Yet, the independently binned outer galaxies (Bin 2) have a much higher dispersion than the inner galaxies in Bin 1. This increase in velocity dispersion in the outer region is hinted at by the outer cumulative galaxy bins which exhibits a sharp upturn beginning near 1400 kpc. This sharp change in velocity dispersion, and subsequently, the mass (see Section 3), does not coincide with the addition of galaxies in the M83 group, which begins in the cumulative galaxy bin 18 or with the large spiral, NGC 5236, is added in the cumulative galaxy bin 27 plotted at the radial value of 907 kpc. The upturn in velocity dispersion is likely to be due to the non-virialization of the outer galaxies (refer to the discussion in Section 3.2).

The solid line in Fig. 5 represents a standard dark matter halo model fit to the data

(Navarro, Frenk, & White 1997, hereafter NFW), nicely tracing the dispersion of the halo of NGC 5128 and the *inner* galaxies of the Centaurus group as well, for a scale radius,  $r_s = 14$  kpc. However, the entire Centaurus group over all radii and halo of NGC 5128 cannot be fit by a single NFW curve. That is, the group as a whole likely has a density profile that is shallower than  $R^{-3}$  at large radius.

The only other direct kinematic comparison between the GCS of a dominant galaxy with its surrounding satellite galaxies is for M87 in the Virgo cluster by Côté et al. (2001). Côté et al. (2001) showed the velocity dispersions of the halo GCs in M87 and the satellite galaxies clearly matched their constructed 2-component mass model for the Virgo cluster. But, unlike our results for NGC 5128 and the Centaurus group, the Virgo galaxies have a dispersion that is much higher than the GCs in the M87 halo. These results are not surprising because M87 and the Virgo cluster contain a large X-ray halo, tracing the large dark matter component in the Virgo cluster that dominates the potential well beyond the halo itself. In the Centaurus group, we clearly do not see this same effect of a very massive, extended outer component to the same degree.

### 3. Mass Determination

The total mass,  $M_t$  of NGC 5128 and the Centaurus group can be determined by the addition of the mass components supported by rotation,  $M_r$ , and random internal motion (“pressure”),  $M_p$ ,

$$M_t = M_p + M_r. \quad (3)$$

The mass supported by pressure was determined here by the Tracer Mass Estimator, developed by Evans et al. (2003) as a generalized projected mass estimator that determines the mass enclosed within the outermost object in the sample. The (spherically symmetric) tracer population, in the Tracer Mass estimator, does not necessarily follow the same mass profile as the system. Although the Tracer Mass Estimator is not the typically selected mass estimator to determine galaxy group mass, it allows a direct comparison with the masses determined from the globular clusters. The pressure supported mass in the Tracer Mass Estimator formulation is

$$M_p = \frac{C}{GN} \sum_i (v_{f_i} - v_{sys})^2 R_i \quad (4)$$

where  $N$  is the number of objects in the sample and  $v_{f_i}$  is the radial velocity of the tracer object with the rotation calculated in Section 2 removed. For an isotropic population of

tracer objects, assumed in this study, the value of C is

$$C = \frac{4(\alpha + \gamma)(4 - \alpha - \gamma)(1 - (\frac{r_{in}}{r_{out}})^{(3-\gamma)})}{\pi(3 - \gamma)(1 - (\frac{r_{in}}{r_{out}})^{(4-\alpha-\gamma)})} \quad (5)$$

where  $r_{in}$  and  $r_{out}$  are the 3-dimensional radii corresponding to the 2-dimensional projected radii ( $R_{in}$  and  $R_{out}$ ) of the innermost and outermost tracers in the sample. The value of  $\gamma$  is defined as the slope of the volume density distribution,

$$\rho(r) \propto (\frac{1}{r})^\gamma, r_{in} \lesssim r \lesssim r_{out}. \quad (6)$$

$\gamma$  is found by determining the surface density slope of the sample and deprojecting the slope to three-dimensions in order to obtain the volume density slope. In Equation 5,  $\alpha$  describes the potential of the system, and is set to zero in this study representing an isothermal halo potential in which the system has a flat rotation curve at large distances. Assuming isotropy in an anisotropic system can, however, overestimate or underestimate the mass by 30% for plausible ranges in anisotropy (Evans et al. 2003).

Another contributor to the uncertainty in the pressure supported mass is from the values assumed for  $r_{in}$  and  $r_{out}$ . Evans et al. (2003) suggest that  $r_{in} \simeq R_{in}$  and  $r_{out} \simeq R_{out}$  for distributions taken over a wide angle (i.e. covering the outer halo reasonably well). However, these approximations when taken at intermediate radial ranges within the distribution lead to an underestimate of the determined mass since the true  $r_{out}$  can be quite a bit larger than  $R_{out}$ . I have estimated the necessary correction factors for the values of  $r_{in}$  and  $r_{out}$  by generating Monte Carlo distributions of both the GCS of NGC 5128, and the group environment. For the GCS of NGC 5128, 340 globulars were randomly placed in a spherically symmetric system extending out to 50 kpc with a  $r^{-2}$  projected density. The distributions were binned in 0-5, 5-10, 10-15, 15-25, 25-50, and 0-50 kpc. For the satellite group of galaxies, a similar spherically symmetric distribution of galaxies was generated for each subgroup in Table 3. The smallest and largest 3-dimensional and projected radii were determined in each radial bin and used to calculate the value of C in Equation 5 for the real positions and the projected positions. I used a total of 500 simulated systems. The correction factors,  $M_{corr}$ , are multiplied onto all the pressure supported component masses in this study, and are shown in Table 1 for the GCs. The correction factors for the galaxies are quite small, as expected, falling between values of 1 and 1.3.

A recent study by Yenko et al. (2006) shows the use of mass estimators, such as the Tracer Mass Estimator, can lead to incorrect mass estimates of up to  $\sim 20\%$  by neglecting substructure within the system in question. For the sample sizes used in this study, any such uncertainties are less than the uncertainties claimed for anisotropic orbital motion and the statistical uncertainty in  $M_p$  itself.



The mass component supported by rotation was calculated from the rotational component of the Jeans Equation,

$$M_r = \frac{R_{out}v_{max}^2}{G} \quad (7)$$

where  $R_{out}$  is the outermost tracer radius in the sample and  $v_{max}$  is the rotation amplitude, calculated in Section 2. These  $M_r$  values are listed in Tables 2 & 3.

### 3.1. The Globular Cluster System of NGC 5128

The mass of NGC 5128 follows from its tracer population of GCs by determining the surface density of the GCS and deprojecting the slope from 2-dimensions to 3-dimensions. The surface density distribution of the entire GCS was determined by binning the known clusters into circular annuli of equally populated bins, giving each bin the same statistical weight to minimize biases (Maíz Apellániz & Úbeda 2005), although, as noted above, the distribution may still have *spatial* biases in favor of the major axis at large radii. The profile is shown in Figure 6. In the innermost region, within 5 kpc, there is incompleteness due to the obscuration of the dust lane and this region is therefore excluded from the mass determination. The surface density fits well to a power law outside of 5 kpc with a slope of  $-2.65 \pm 0.17$  (reduced  $\chi^2 = 0.04$  from a Marquardt-Levenberg fitting routine from Press et al. 1992). A value of  $\gamma = 3.65$ , was then used in the mass calculations.

The rotationally supported mass was calculated from Equation 7, and the determined rotation amplitude in each bin shown in Table 1. The determined masses are actually lower limits as the inclination angle of the true rotation axis with the plane of the sky is not known. Peng, Ford, & Freeman (2004) argue, using planetary nebula data, that NGC 5128 is triaxial in nature and is viewed nearly edge-on. If so, the rotation measured would be a good estimate of the true rotation of the system. In any case,  $M_r$  is small compared with the pressure component,  $M_p$ .

The total mass of the system determined within the outermost cluster in each bin is listed in Table 1.

### 3.2. The Centaurus Group Mass

The mass was determined separately for the 13 *confirmed* Centaurus group members, the M83 group members, the two independent bins of galaxies (Bin 1 and Bin 2), and for the larger number of probable satellites with each additional satellite galaxy added in increasing

radial projection from NGC 5128. The adopted value of  $\gamma$  was determined independently for each list of galaxies in the same manner as was done for the GCS in Section 3.1, with typical values ranging from  $\gamma = 1.5$  to  $\gamma = 3.2$ . The calculated masses with projection corrections, are shown in Tables 2 & 3 and are plotted in Figure 7.

The mass calculation for the group cannot be continued out indefinitely far because at some radius, the fundamental assumption of virial equilibrium breaks down. At very large radii, the group has not had enough time to undergo full relaxation (Côté et al. 1997). The dynamical and crossing times (Binney & Tremaine 1987), when set equal to a Hubble time, occur at radii of 1967 kpc and 1400 kpc, respectively, for the entire 62 galaxies surrounding NGC 5128. Similarly, Karachentsev et al. (2006) found a "surface of zero velocity" around Centaurus of 1440 kpc, coinciding with the upturn in velocity dispersion noted by the cumulative galaxy bins seen in Fig. 5 and discussed in Section 2.3. Thus an appropriate radial limit for the mass calculation is  $R \simeq 1.5$  Mpc. Thus, the large masses determined for the outer 15-20 galaxies, (includes Bin 2 and cumulative galaxy bins 42-62) are not valid as they are not likely virialized objects in the system. This is carried through to the mass-to-light ratios determined for these outer objects in Section 3.3.

### 3.3. Mass-to-Light Ratios

The mass-to-light ratios were calculated from the total mass,  $M_t$ , determined in Section 3 and a B-band luminosity and galactic extinction for each galaxy from Karachentsev et al. (2004).

All mass-to-light ratios are listed in Tables 2 & 3. The B-band luminosity for the galaxy calculations include all of the galaxies within the outermost radii of each bin. The M83 complex, therefore, contributes to the luminosity of Bin 1 and Bin 2 in Table 2, although it is not included as part of the mass tracer population. The B-band luminosity of NGC 5128 is  $3.79 \pm 0.01 \times 10^{10} L_{\odot}$ . This single galaxy makes up 66% of the entire light of the Centaurus group of galaxies. The mass-to-light ratio of NGC 5128 alone is  $52 \pm 22 M_{\odot}/L_{\odot}$  out to  $R = 45$  kpc.

The mass of the Centaurus group of galaxies is determined from this study to be  $(9.2 \pm 3.0) \times 10^{12} M_{\odot}$  out to the dynamical radius, leading to  $M/L_B = 153 \pm 50 M_{\odot}/L_{\odot}$ . These values are quite comparable to the most recent study of Karachentsev et al. (2006) who determined the orbital mass of the Centaurus group to be  $7.5 \times 10^{12} M_{\odot}$ , the virial mass  $8.9 \times 10^{12} M_{\odot}$ , and the mass determined within a zero-velocity surface including dark energy  $6.4 \pm 1.8 \times 10^{12} M_{\odot}$ . Karachentsev et al. (2006) also determined a  $M/L_B = 137 M_{\odot}/L_{\odot}$ .

The  $M/L_B$  ratio for the Centaurus group is larger than many other groups of galaxies in the nearby universe ( $M/L_B = 8 - 88 M_\odot/L_\odot$  (Karachentsev 2005)), but mass-to-light ratios are typically larger for groups dominated by giant ellipticals, compared to spiral dominated groups, such as the Milky Way ( $M/L_B = 28 - 29 M_\odot/L_\odot$ ), IC342 ( $M/L_B = 18 - 30 M_\odot/L_\odot$ ), or M81 ( $M/L_B = 19 - 32 M_\odot/L_\odot$ ) (Karachentsev 2005).

#### 4. Bounding Argument

In brief, the satellite galaxies in the Centaurus group strongly indicate a possible connection to the halo system of its central group member. The *confirmed* members in both the Centaurus and M83 groups, with their brightest members separated by a projected radius of 1 Mpc, have many surrounding galaxies with distances and/or radial velocities that do not have confirmed group membership. It seems a possibility that these two groups resemble the Milky Way and M31 as bound systems. Exploring this idea leads to the application of a simple Newtonian bounding argument, used recently by Brough et al. (2006), Cortese et al. (2004), and others. If the two groups, Centaurus and M83, are part of a larger system, then the inequality

$$\frac{v_r^2 R_p}{2} \leq GM \sin^2(\beta) \cos(\beta) \quad (8)$$

holds. In Equation 8,  $M = M_{83_{group}} + C_{en_{group}} = (9.65 \pm 3.01) \times 10^{12} M_\odot$  is the total mass of the confirmed system,  $v_r = 25 \text{ km s}^{-1}$  is the relative velocity between the two groups,  $R_p = 907 \text{ kpc}$  is the projected distance between the centroids of the two groups, and  $\beta$  is the projection angle between the plane of the sky and the line that joins the centers of the two groups. The inequality in Equation 8 holds for all projected angles between  $5^\circ \leq \beta \leq 89^\circ$ , using the observed radial velocities of the Centaurus group and M83 centroids to be those of NGC 5128,  $541 \text{ km s}^{-1}$ , and NGC 5236,  $516 \text{ km s}^{-1}$ , respectively. The probability that Centaurus and M83 are bound can then be calculated from

$$P_{bound} = \int_{\beta_1}^{\beta_2} \cos(\beta) d\beta \quad (9)$$

(Girardi et al. 2005). I find that the probability that these systems are bound is at the 91% level.

#### 5. Discussion and Summary

Investigating the kinematics of the GCs in the giant elliptical galaxy, NGC 5128, and the kinematics of over 60 satellite galaxies in and surrounding the Centaurus group, has shown

interesting new results. The rotation amplitude, rotation axis, and velocity dispersion of both the halo of NGC 5128 and surrounding galaxies both have means of  $\Omega R = 67 \pm 27$  km s<sup>-1</sup>,  $\Theta_o = 162 \pm 22^\circ$  E of N, and  $\sigma_v = 103 \pm 14$  km s<sup>-1</sup>. The masses determined with the Tracer Mass Estimator and the spherical component of the Jeans Equation, lead to projection corrected masses of  $(1.3 \pm 0.5) \times 10^{12} M_\odot$  for NGC 5128 and  $(9.2 \pm 3.0) \times 10^{12} M_\odot$  for the entire Centaurus group. Mass-to-light ratios in the B-magnitude were subsequently determined to be  $52 \pm 22 M_\odot/L_\odot$  for NGC 5128 and  $153 \pm 50 M_\odot/L_\odot$  for the Centaurus group.

The similar kinematics between the halo of the brightest group member with its surrounding satellites suggests that the halo of NGC 5128 could therefore be thought of as the innermost component of the entire group that surrounds it.

The Centaurus group is likely bound, although its outer regions are unlikely to be virialized beyond  $R \simeq 1.5$  Mpc. The global dynamics of the group that we are seeing, could therefore represent the initial internal shear of the pregalactic filamentary structure from which it condensed. NGC 5128 could have formed early on as a galaxy that was already centrally dominant, and now continues to build up by a series of minor mergers and accretions, leading to an averaging of the kinematics from the surrounding satellite galaxies that we now measure in the GCs in the NGC 5128 halo. A single or small number of major merger events would not necessarily produce these kinematic similarities. This view is consistent with the recent work on the halo stars in NGC 5128 which have a mean age of  $8_{-3.5}^{+3}$  Gyr (Rejkuba et al. 2005), and the age distribution of the GCs which shows that a high fraction of both metal-rich and metal-poor GCs are old (M. Beasley et al. 2006, in preparation). It would be interesting to extend this type of study to other nearby groups with centrally dominant giants, although large samples of GCs and satellite galaxies with measured radial velocities are required in each case.

K.A.W. would like to thank Willam E. Harris and James Wadsley from McMaster University for their helpful suggestions and many insightful discussions, as well as Mike Beasley for transmitting cluster velocity data in advance of publication. K.A.W. would also like to thank the referee who provided very thorough comments on this paper. This research was funded by NSERC through grants to W.E.H.

## REFERENCES

- Binney, J., & Tremaine, S. 1987, *Galactic Dynamics* (Princeton, NJ: Princeton University Press)
- Brainerd, T.G. 2005, *ApJ*, 628, L101
- Brough, S., Forbes, D.A., Kilborn, V.A., Couch, W., & Colless, M. 2006, preprint (astro-ph/0603778)
- Cortese, L., Gavazzi, G., Boselli, A., Iglesias-Paramo, J., & Carrasco, L. 2004 *A&A*, 425, 429
- Côté, P., McLaughlin, D.E., Hanes, D.A., Bridges, T.J., Geisler, D., Merritt, D., Hesser, J.E., Harris, G.L.H., & Lee, M.G. 2001, *ApJ*, 559, 828
- Côté, S., Freeman, K.C., Carignan, C., & Quinn, P.J. 1997, *AJ*, 114, 1313
- de Vaucouleurs, G. 1961, *ApJS*, 5, 233D
- Dufour, R.J., Harvel, C.A., Martins, D.M., Schiffer, F.H., Talent, D.L., Wells, D.C., van den Bergh, S., & Talbot, R.J. 1979, *AJ*, 84, 284
- Evans, N.W., Wilkinson, M.I., Perrett, K.M., & Bridges, T.J. 2003, *ApJ*, 583, 752
- Girardi, M., Demarco, R., Rosati, P., & Borgani, S. 2005, *A&A*, 442,29
- Girardi, M., Mardirossian, F., Marinoni, C., Mezzetti, M., & Rigoni, E. 2003, *A&A*, 410, 461
- Heisler, J., Tremaine, S., & Bahcall, J.N. 1985, *ApJ*, 298, 8H
- Hui, X., Ford, H.C., Freeman, K.C., & Dopita, M.A. 1995, *ApJ*, 449, 592
- Karachentsev, I.D., Sharina, M.E., Dolphin, A.E., Grebel, E.K., Geisler, D., Guhathakurta, P., Hodge, P.W., Karachentseva, V.E., Sarajedini, A., & Seitzer, P. 2002, *A&A*, 385, 21
- Karachentsev, I.D., Karachentseva, V.E., Huchtmeier, W.K., & Makarov, D.I. 2004, *AJ*, 127, 2031
- Karachentsev, I.D. 2005, *AJ*, 129, 178

- Karachentsev, I.D., Tully, R.B., Dolphin, A., Sharina, M., Makarova, L., Makarov, D., Kashibadze, O.G., Karachentseva, V., Sakai, S., Shaya, E.J., & Rizzi, L. 2006, preprint (astro-ph/0603091)
- Maíz Apellániz, J. & Úbeda, L. 2005, *ApJ*, 629, 7873
- Navarro, J.F., Frenk, C.S., & White, S.D.M. 1997, *ApJ*, 490, 493
- Peng, E.W., Ford, H.C., & Freeman, K.C. 2004, *ApJS*, 150, 367
- Peng, E.W., Ford, H.C., & Freeman, K.C. 2004, *ApJ*, 602, 685
- Peng, E.W., Ford, H.C., & Freeman, K.C. 2004, *ApJ*, 602, 705
- Press, W.H., Teukolsky, S.A., Vetterling, W.T., & Flannery, B.P. 1992, *Numerical Recipes in Fortran* (2nd Ed., Cambridge: Cambridge University Press)
- Pryor, C. & Meylan, G. 1993, in *ASP Conf. Ser. 50: Structure and Dynamics of Globular Clusters*, 357
- Rejkuba, M. 2004, *A&A*, 413, 903
- Rejkuba, M., Greggio, L., Harris, W.E., Harris, G.L.H., & Peng, E.W. 2005, *ApJ*, 631, 262
- Richtler, T., Dirsch, B., Gebhardt, K., Geisler, D., Hilker, M., Alonso, M. V., Forte, J. C., and Grebel, E. K., Infante, L., Larsen, S., Minniti, D., & Rejkuba, M. 2004, *AJ*, 127, 2094
- Warnick, K., & Knebe, A. 2005, preprint (astro-ph/0512156)
- Weinmann, S.M., van den Bosch, F.C., Yang, X., & Mo, H.J. 2006, *MNRAS*, 366, 2
- Woodley, K.A., Harris, W.E., & Harris, G.L.H. 2005, *AJ*, 129, 2654
- Yang, X., van den Bosch, F.C., Mo, H.J., Mao, S., Kang, X., Weinmann, S.M., Guo, Y., & Jing, Y.P. 2006, preprint (astro-ph/0601040)
- Yencho, B.M., Johnston, K.V., Bullock, J.S., & Rhode, K.L. 2006, *ApJ*, 643, 154
- Zentner, A.R., Kravtsov, A.V., Gnedin, O.Y., & Klypin, A.A. 2005, *ApJ*, 629, 219

Table 1. Kinematic and Dynamic Solutions for the Globular Cluster System of NGC 5128

Radial Bin (kpc)	$R_{mean}$ (kpc)	$R_{out}$ (kpc)	N	$\Omega R$ (km s <sup>-1</sup> )	$\Theta_o$ (° E of N)	$\sigma_v$ (km s <sup>-1</sup> )	$M_{corr}$	$M_p$ ( $\times 10^{10} M_\odot$ )	$M_r$ ( $\times 10^{10} M_\odot$ )	$M_t$ ( $\times 10^{10} M_\odot$ )
0-50	12.9	48.8	343	40±10	189±12	123±6	1.0	125.8±46.5	3.1±1.3	128.9±46.5
0-5	3.64	4.98	55	24±21	334±59	120±13	-	-	-	-
5-10	7.65	9.96	124	43±15	195±20	112±8	2.3	37.4±6.4	0.4±0.3	37.8±6.4
10-15	12.4	14.9	68	83±25	195±12	105±11	1.6	36.5±9.3	2.4±1.5	38.9±9.4
15-25	19.0	24.3	57	35±26	183±34	147±16	1.3	89.5±27.4	0.7±1.0	90.2±27.4
25-50	34.7	48.8	39	96±45	169±17	148±22	1.0	184.7±84.5	10.4±9.8	195.1±85.1

Table 2. Kinematic and Dynamic Solutions for the Centaurus Group, M83 Group, and Radially Binned Galaxies Surrounding NGC 5128

Bin	$R_{mean}$ (kpc)	$R_{out}$ (kpc)	$\Omega R$ (km s <sup>-1</sup> )	$\Theta_o$ ( <sup>o</sup> E of N)	$\sigma_v$ (km s <sup>-1</sup> )	$\gamma$	$M_p$ ( $\times 10^{11} M_{\odot}$ )	$M_r$ ( $\times 10^{11} M_{\odot}$ )	$M_t$ ( $\times 10^{11} M_{\odot}$ )	$L_B$ ( $\times 10^{10} L_{\odot}$ )	$M/L$ ( $M_{\odot}/L_{\odot}$ )
M83	119.1 <sup>a</sup>	237.1 <sup>a</sup>	25±27	299±88	53±16	1.79±0.67	4.7±2.7	0.3±0.7	5.0±2.8	4.0	12±1
Cen	358.5	810.1	125±50	159±23	115±25	2.23±0.31	62.1±18.7	29.5±23.6	91.5±30.1	6.0	153±1
Bin 1 <sup>b</sup>	539.5	1099.1	67±30	156±24	98±15	2.01±0.10	69.5±6.2	11.6±10.3	81.1±12.0	10.0	81±1
Bin 2 <sup>c</sup>	2594.2	4727.75	36±58	108±50	179±26	3.17±0.40	1052±363	14.1±45.7	1066±366	13.9	765±2

<sup>a</sup>The projected radius from NGC 5236.

<sup>b</sup>Bin 1 includes the 27 galaxies nearest NGC 5128 with radial velocities, excluding the M83 group.

<sup>c</sup>Bin 2 includes the 28<sup>th</sup> to 53<sup>rd</sup> nearest galaxies to NGC 5128 with radial velocities, excluding the M83 group.



Table 3. Kinematic and Dynamic Solutions for the Cumulatively Binned Galaxies Surrounding NGC 5128

N	$R_{out}$ (kpc)	$\Omega R$ (km s <sup>-1</sup> )	$\Theta_o$ ( <sup>o</sup> E of N)	$\sigma_v$ (km s <sup>-1</sup> )	$\gamma$	$M_p$ ( $\times 10^{11} M_\odot$ )	$M_r$ ( $\times 10^{11} M_\odot$ )	$M_t$ ( $\times 10^{11} M_\odot$ )	$L_B$ ( $\times 10^{10} L_\odot$ )	$M/L_B$ ( $M_\odot/L_\odot$ )
14	484.5	74±38	157±32	90±20	1.56±0.11	20.1±1.6	6.2±6.3	26.3±6.5	4.1	64±16
17	653.9	76±35	155±31	92±17	1.52±0.08	27.3±1.6	8.8±8.1	36.1±8.3	5.4	66±15
20 <sup>d</sup>	757.0	72±33	152±28	93±16	1.83±0.02	35.2±1.0	9.1±8.4	44.3±8.4	5.5	79±15
23 <sup>d</sup>	795.5	77±31	153±22	90±15	1.83±0.02	35.0±1.0	11.0±8.8	46.0±8.9	5.7	80±15
26 <sup>d</sup>	862.4	88±29	154±17	87±13	1.53±0.29	34.8±7.0	15.6±10.3	50.3±12.4	5.7	87±21
29 <sup>d</sup>	948.2	86±28	156±16	84±12	1.75±0.30	35.9±8.1	16.3±10.6	52.3±13.3	9.7	54±13
32 <sup>d</sup>	976.5	68±24	143±20	87±12	1.75±0.30	42.3±9.5	10.5±7.4	52.8±12.1	9.7	54±12
35 <sup>d</sup>	1069.5	64±25	154±20	88±12	1.68±0.22	45.7±7.4	10.2±8.0	55.9±10.9	9.7	57±11
38 <sup>d</sup>	1300.2	61±25	159±19	90±12	1.68±0.22	53.6±8.6	11.3±9.2	64.8±12.6	9.8	66±12
41 <sup>d</sup>	1488.1	61±23	164±18	88±12	1.68±0.22	56.4±9.1	12.9±9.7	69.3±13.3	9.9	69±13
44 <sup>d</sup>	1728.8	69±23	175±15	91±11	1.94±0.29	71.5±18.1	19.2±12.8	90.6±22.2	13.1	69±16
47 <sup>d</sup>	1874.2	71±24	185±15	97±12	1.94±0.29	92.8±23.6	22.0±14.9	114.8±27.9	13.2	87±21
50 <sup>d</sup>	2486.4	69±23	188±15	99±11	2.25±0.32	139.0±47.6	27.6±18.4	166.5±50.99	13.7	121±37
53 <sup>d</sup>	2767.2	47±24	191±24	104±11	2.25±0.32	210.5±72.5	14.2±14.5	224.7±73.93	13.8	162±53
56 <sup>d</sup>	3572.3	49±26	177±24	117±11	2.57±0.28	490.6±218.6	20.0±21.2	510.6±219.7	13.8	368±158
59 <sup>d</sup>	4041.1	41±27	158±31	117±11	2.47±0.28	653.5±251.4	15.8±20.8	669.3±252.3	13.9	481±181
62 <sup>d</sup>	4727.8	44±27	137±32	137±12	2.47±0.28	869.8±337.8	21.3±26.2	891.1±338.8	13.9	640±243

<sup>d</sup>Includes confirmed galaxies from the M83 group.

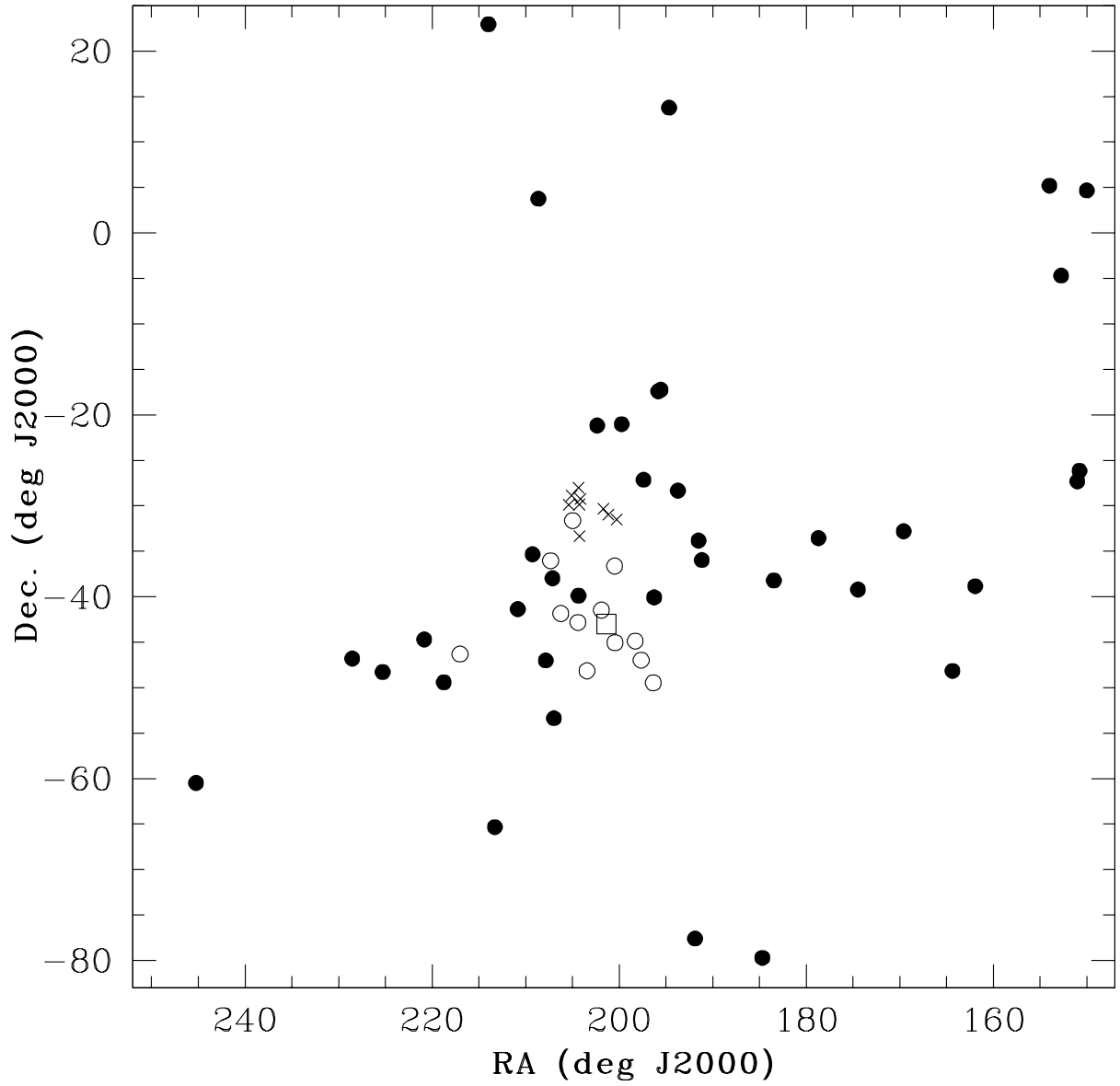


Fig. 1.— The positions of galaxies surrounding NGC 5128 with available radial velocity measurements. NGC 5128 is the *open square*, the confirmed galaxies in the Centaurus group are *open circles*, the confirmed members in the M83 group are *crosses*, and the surrounding galaxies that are not confirmed to belong to either the Centaurus or M83 groups are *solid circles*.

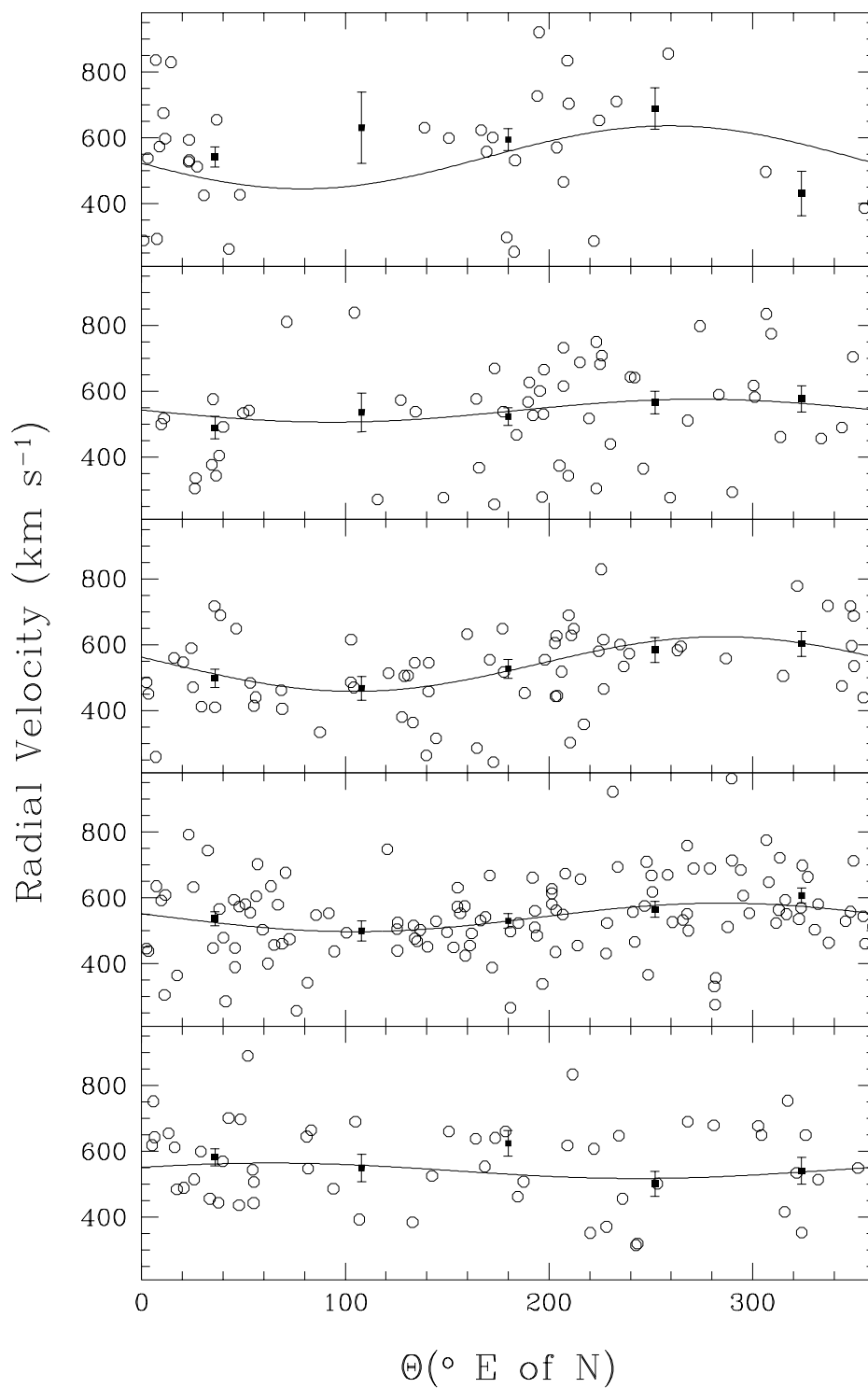


Fig. 2.— The sine curve fit for the GCs in NGC 5128 indicated by the *open circles*, binned radially with fixed systemic velocity. The radial bins are (*bottom panel*) 0-5 kpc, (*2<sup>nd</sup> panel*) 5-10 kpc, (*3<sup>rd</sup> panel*) 10-15 kpc, (*4<sup>th</sup> panel*) 15-25 kpc, and (*top panel*) 25-50 kpc. The *solid squares* are the weighted velocities in  $72^\circ$  bins.

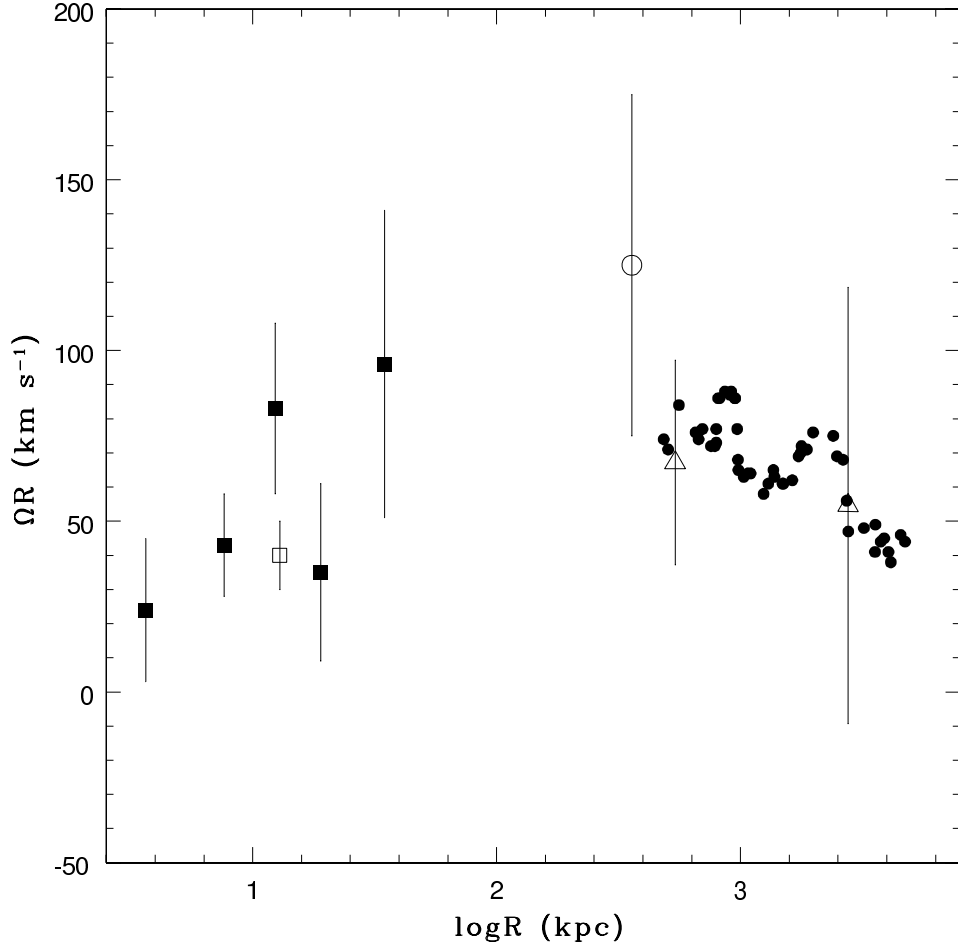


Fig. 3.— Rotation amplitude,  $\Omega R$ , as a function of projected radius from the center of NGC 5128 plotted for the 343 GCs in NGC 5128 (*open square*), and in independent radial bins (*closed squares*), see Table 1). Also plotted are the confirmed galaxy members from the Centaurus group in Karachentsev et al. (2002) (*open circle*), with the cumulative addition of other probable satellite galaxies in angular distance from NGC 5128 (*closed circles*), including the M83 group, see Table 3. The galaxies are also independently binned for the nearest 27 galaxies from NGC 5128 in projected radius (Bin 1), and then the following 26 galaxies in the next bin (Bin 2) (*open triangles*), excluding the M83 group. The mean rotation amplitude is  $67 \pm 27 \text{ km s}^{-1}$  for the cumulative galaxy points. The radial values plotted are the average of the objects in each bin, with the exception of the additive galaxy points (*solid circles*), which are plotted at the radial position of the last galaxy in each bin.

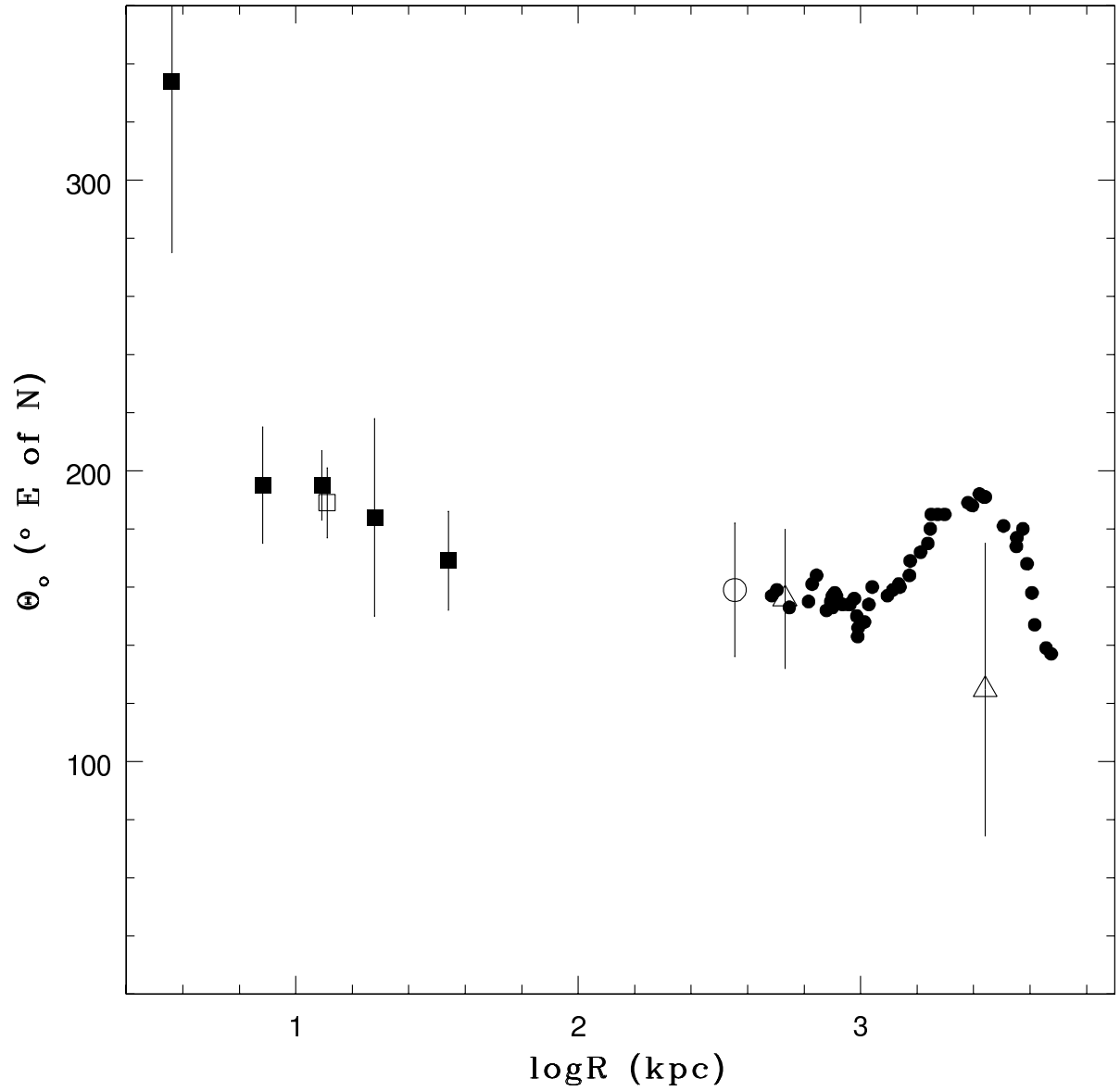


Fig. 4.— Rotation axis,  $\Theta_o$ , measured in degrees East of North, as a function of projected radius from the center of NGC 5128. Symbols are the same as in Fig. 3. The mean rotation axis is  $163 \pm 22^{\circ}$  E of N for the cumulative galaxy points. The radial values plotted are the average of the objects in the each bin, with the exception of the additive galaxy points (*solid circles*), which are plotted at the radial position of the last galaxy in each bin.

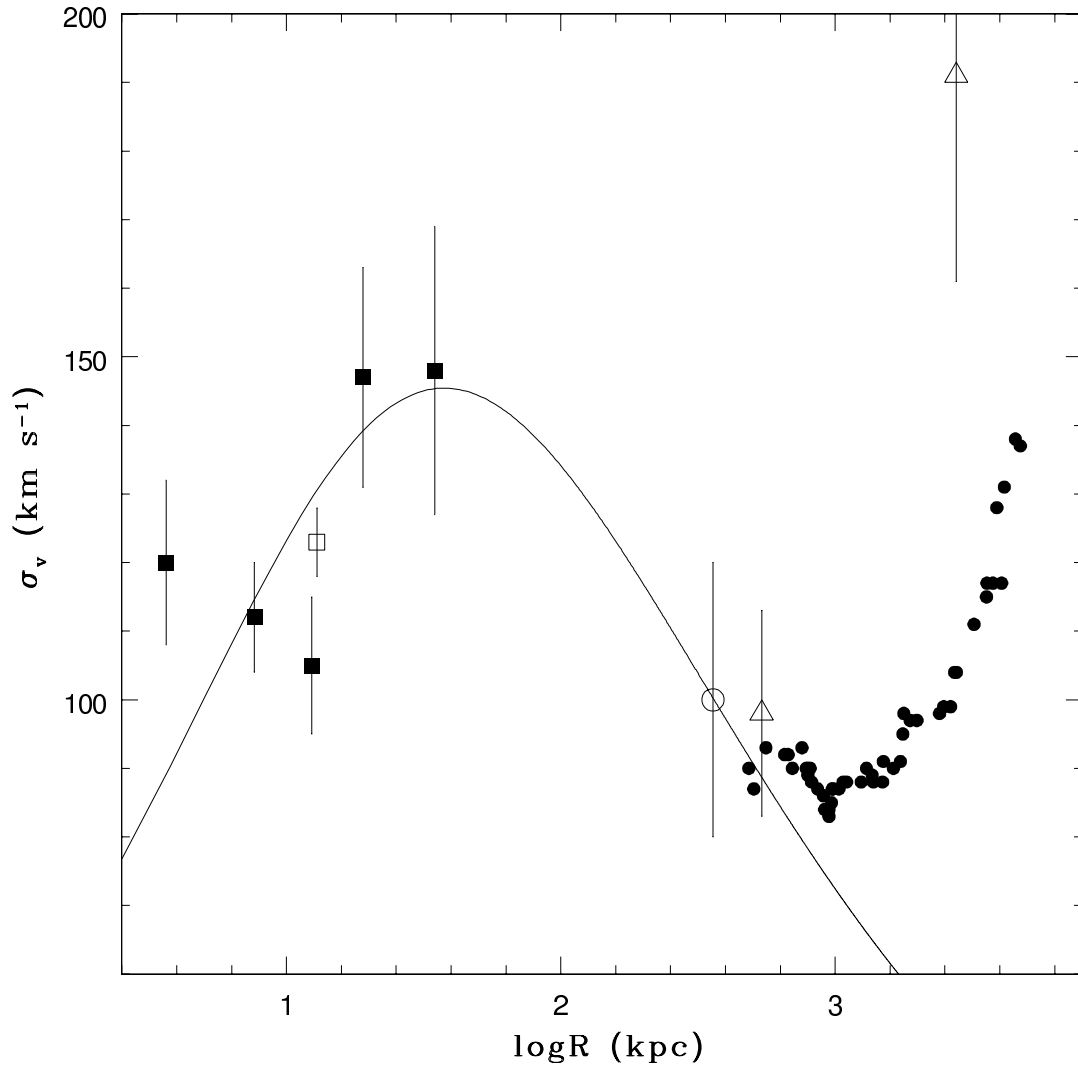


Fig. 5.— The velocity dispersion,  $\sigma_v$ , as a function of radius from the center of NGC 5128. The symbols are the same as in Fig. 3. The average velocity dispersion of all points is  $103 \pm 14$  km s<sup>-1</sup>. The solid line is the dark matter halo fit using an NFW model with a scale radius of 14 kpc. The outermost galaxies are not believed to be virialized (see Section 3.2 for details). The radial values plotted are the average of the objects in each bin, with the exception of the additive galaxy points (*solid circles*), which are plotted at the last galaxy’s radial position.

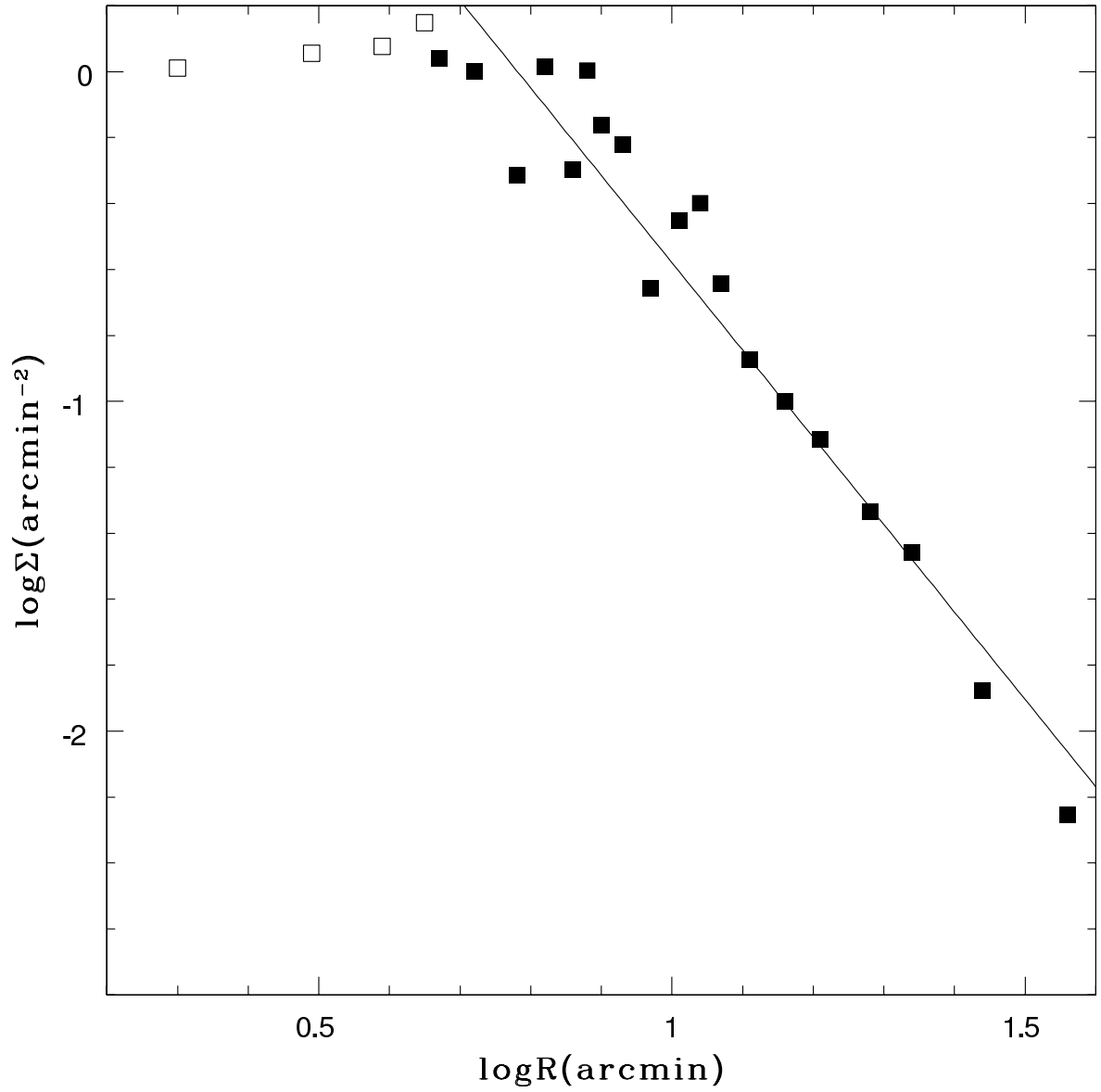


Fig. 6.— The surface density,  $\Sigma$ , of the GCs in NGC 5128 as a function of galactocentric radius. Each bin is equally weighted and fit to a power law with slope  $-2.65 \pm 0.17$ . Data less than 5 kpc from the galaxy center (*open circles*) has been ignored for the fit.

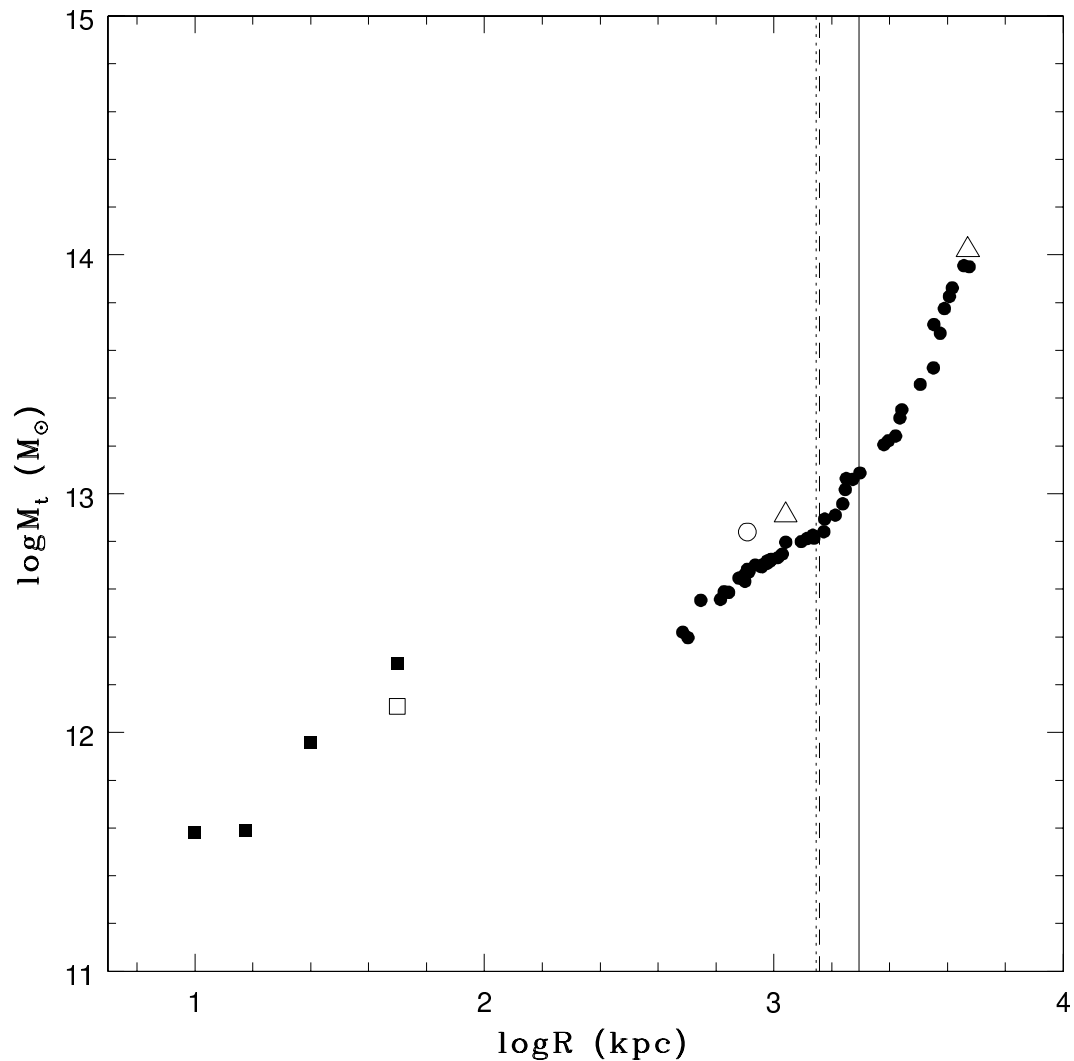


Fig. 7.— The determined total masses as a function of radius from the center of NGC 5128. The symbols are the same as in Fig. 3. The average mass determined by the cumulative galaxies is  $5.7 \times 10^{12} M_{\odot}$ . The radii for the dynamical and crossing timescales equal to a Hubble time are shown as solid and dashed lines, respectively, for all 62 galaxies. The dotted line is the zero velocity surface determined by Karachentsev et al. (2006). The radial values plotted are the last object’s radial position.